

Extreme Ionospheric Storms and Their Impact on WAAS

L. Sparks, A. Komjathy, and A.J. Mannucci

Jet Propulsion Laboratory, California Institute of Technology

E. Altshuler

Sequoia Research Corporation

T. Walter and J. Blanch

Stanford University

M. Bakry El-Arini and R. Lejeune

Mitre Corporation

Abstract

The primary purpose of satellite-based augmentation systems (SBAS) is to provide accurate and reliable differential corrections of Global Positioning System (GPS) measurements for aircraft navigation. The Wide Area Augmentation System (WAAS) relies on a threat model to protect users from erroneous signal delay estimates that arise as a consequence of undersampling ionospheric irregularities. We examine the impact of *extreme* ionospheric storms on the threat model and discuss how implementing an extreme storm detector in WAAS can result in improved safety and availability.

I. Introduction

The largest source of positioning error for single-frequency users of the Global Positioning System (GPS) is typically the radio delay caused by the ionosphere. To allow the user to compensate for this error, the Wide Area Augmentation System (WAAS) broadcasts both estimates of ionospheric delay and error bounds that circumscribe the uncertainty in these estimates. However, when observations by receivers in the WAAS reference station network fail to sample adequately the presence of irregularities in the ionosphere, erroneous delay estimates can result. To protect the user from such errors, WAAS relies on an *ionospheric threat model* (Sparks *et al.*, 2001; Altshuler *et al.*, 2001) derived from analysis of post-processed WAAS data obtained under disturbed conditions. The threat model contains tabulated corrections that augment the confidence bound of the estimated delay to account for the worst-case threat posed by irregularities that escape detection. It has been found that the dominant contributions to the threat model come from recovery periods that follow the onset of highly disturbed conditions associated with *extreme ionospheric storms*. The occurrence of such storms generally coincides with a strong drop in the geomagnetic D_{st} index. The observed total electron content is characterized by unusually large magnitudes and strong gradients over an extensive geographic region. The extreme storm that occurred over the last three days of October of 2003, for example, generated vertical delay values at mid-latitudes that exceeded 200 TECU (where 1 TECU corresponds to 10^{16} electrons per meter²). Storms of such magnitude occur only rarely over the course of a solar cycle (*e.g.*, 5 – 10 times per 11-year cycle). This paper examines the impact of extreme storms on the WAAS ionospheric threat model and how this impact can be mitigated to provide improved system safety and availability.

Under its initial operating capability (IOC), WAAS broadcasts confidence bounds whose dominant contribution usually comes from the ionospheric threat model. A significant limitation of the IOC WAAS is that the threat model is always protecting against extreme conditions that, in fact, arise rarely. The threat model assumes the worst possible threat to be present consistent with a given sampling of the ionosphere. While this conservatism ensures a high degree of safety, it also restricts availability. To help achieve the higher performance requirements of the full operating capability

(FOC), it has been proposed to introduce into WAAS an *extreme storm detector* that distinguishes extreme storms from moderate ones. By relying on such a detector to notify the system whenever an extreme storm occurs, the threat model can be reserved for addressing only those threats posed by less severe storms. Restricting the threat model to moderate storms should permit a reduction in the amount by which the broadcast confidence bounds are augmented to account for undersampling, and, as a consequence, WAAS availability should improve significantly relative to performance with the same threat model in the absence of an extreme storm detector.

Implementing an extreme storm detector in WAAS has implications for system safety as well. The protection provided by the IOC threat model is based largely upon the extreme storms that occurred prior to the commissioning of WAAS in July of 2003. The nature of the IOC threat model methodology implies that any subsequent storm of greater magnitude than those already incorporated into the threat model would require its re-computation to include these new data. Such an event has, in fact, occurred. A threat model that includes data from Halloween 2003 storm is significantly more conservative than the IOC threat model. It is important to note, however, that WAAS performed well during this storm (*i.e.*, no user position estimate was found to lie outside the error limits derived from the broadcast confidence bounds of the delay estimate). Nevertheless, the implementation of an extreme storm detector would provide an added measure of protection against the impact of any future storm that is significantly larger than those observed previously and would obviate the need to regenerate the threat model based upon new data.

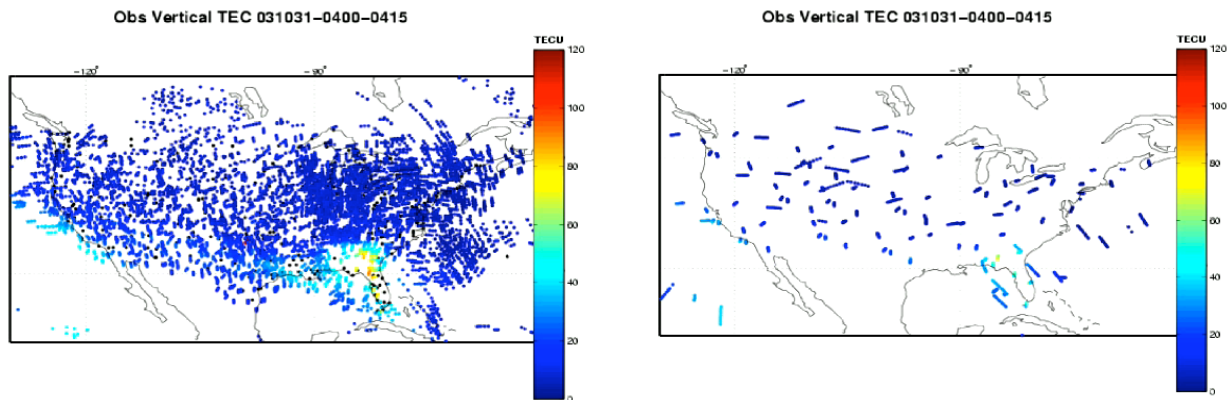


Fig. 1. (a) The vertical ionospheric delay (in TECU) over the southeastern United States between 4:00 and 4:15 UTC, October 31, 2003 as sampled by the CORS network. (b) The same delay as sampled by the WAAS network.

Finally, it has been found empirically that the dominant contributions to the threat model arise from disturbances that occur relatively late in the evolution of extreme storms, not near their onsets. An extreme storm detector would provide protection against the impact of certain dense, highly localized structures that have been observed typically one-to-two hours or more following storm onset. Figure 1 shows the vertical delay over the southeastern United States between 4:00 and 4:15 UTC, October 31, 2003 as sampled by (a) receivers in the CORS network and (b) receivers in the WAAS network. Clearly visible in Fig. 1(a) is a localized irregularity over Georgia and northern Florida that nearly escapes detection in Fig 1(b). In part due to structures such as this, WAAS delay estimates are not reliable during extreme storms. An extreme storm detector in WAAS would identify the onset of an extreme storm and determine a period over which delay estimates at all WAAS ionospheric grid points would be declared unusable. If this period extended well beyond the recovery period of the storm, users would be protected from errors arising from a failure to sample irregularities such as those depicted in Fig. 1.

This paper is organized as follows. In Section II, we describe the algorithm for detecting extreme ionospheric storms that is currently being considered for implementation in WAAS. In Section III we examine the impact of this algorithm on the ionospheric threat model. Our results are summarized in Section IV.

II. The Extreme Storm Detector

The proposed algorithm for detecting extreme ionospheric storms is based upon the WAAS irregularity detector. In this section we briefly review algorithms that WAAS uses to estimate ionospheric delay and to detect

ionospheric irregularities, and then we present a metric that may be used to quantify the magnitude of the storm on a regional basis.

A. Ionospheric delay estimation

Slant delay estimates in WAAS are determined from estimates of vertical ionospheric delays modeled at regularly-spaced intervals in latitude and longitude, *i.e.*, at *ionospheric grid points* (IGPs). At each IGP, WAAS determines the vertical ionospheric delay by constructing a planar fit of a set of slant delay measurements projected to vertical. To achieve this projection, WAAS relies on the standard *thin-shell* model of the ionosphere. At an ionospheric pierce point (IPP), *i.e.*, the point where a raypath crosses the shell height h_i , the ratio of slant delay to vertical delay is approximated as

$$\frac{STE C_{IPP}}{VTE C_{IPP}} = \frac{R_e \cos \epsilon}{R_e + h_i} \quad (1)$$

where R_e is the earth radius and ϵ is the satellite elevation angle. All IPPs that reside within a minimum distance R_{min} of the IGP are included in the fit. If the number of IPPs within this fit radius is less than N_{target} , the fit radius R_{fit} is extended until it encompasses N_{target} points. If the fit radius attains a maximum value of R_{max} without encircling N_{target} points, the fit is performed using fewer than N_{target} points, provided this number is greater than or equal to a specified minimum N_{min} . Currently used values for h_i , R_{min} , R_{max} , N_{target} , and N_{min} are, respectively, 350 km, 800 km, 2100 km, 30, and 10.

The WAAS model for vertical ionospheric delay near an IGP can be represented as

$$\mathbf{y} = \mathbf{G} \cdot \mathbf{a} + \mathbf{R} + \mathbf{E}, \quad (2)$$

where \mathbf{y} is a vector of observed slant delay values projected to vertical, $\mathbf{a} = [a_0 \ a_1 \ a_2]^T$ is a vector of coefficients defining the planar trend of the ionospheric delay, \mathbf{G} is a matrix of partial derivatives of vertical delay with respect to the planar trend parameters, \mathbf{R} is a vector describing small delay deviations from the planar trend, and \mathbf{E} is a vector representing measurement error. Each row in \mathbf{G} is of the form $[1 \ d_E \ d_N]$, where d_E and d_N are the distances from the IGP to the IPP in the eastern and northern directions, respectively. A least squares estimate \mathbf{a} is obtained by solving the equation

$$[\mathbf{G}^T \cdot \mathbf{W} \cdot \mathbf{G}] \mathbf{a} = [\mathbf{G}^T \cdot \mathbf{W} \cdot \mathbf{y}], \quad (3)$$

where the inverse of the observation weighting matrix is defined as

$$\begin{aligned} \mathbf{W}^{-1} &= \langle (\mathbf{R} + \mathbf{E})(\mathbf{R} + \mathbf{E})^T \rangle \\ &= \langle \mathbf{R}\mathbf{R}^T \rangle + \langle \mathbf{E}\mathbf{E}^T \rangle. \end{aligned} \quad (4)$$

The final equation above assumes that the small deviations from the planar trend are uncorrelated with the measurement error. Under nominal, *i.e.*, quiet, ionospheric conditions, $\langle \mathbf{R}\mathbf{R}^T \rangle$ may be treated as a diagonal matrix with

$$\langle \mathbf{R}\mathbf{R}^T \rangle = (\overline{\Delta}_{decor}^{nom})^2 \mathbf{I}, \quad (5)$$

where \mathbf{I} is the identity matrix and $\overline{\Delta}_{decor}^{nom}$ characterizes the local spatial decorrelation of the ionospheric vertical delay. This parameter is currently set conservatively to 35 cm, independent of both measurement elevation angle and distance from the IGP. The measurement covariance may be expressed as

$$\langle \mathbf{E}\mathbf{E}^T \rangle = \begin{bmatrix} \overline{\Delta}_{mon,IPP,1}^2 & \overline{\Delta}_{bias,1,2}^2 & \cdots & \overline{\Delta}_{bias,1,N}^2 \\ \overline{\Delta}_{bias,2,1}^2 & \overline{\Delta}_{mon,IPP,2}^2 & \cdots & \overline{\Delta}_{bias,1,N}^2 \\ \vdots & \vdots & \ddots & \vdots \\ \overline{\Delta}_{bias,N,1}^2 & \overline{\Delta}_{bias,N,2}^2 & \cdots & \overline{\Delta}_{mon,IPP,N}^2 \end{bmatrix} \quad (6)$$

where the $\overline{\Delta}_{mon,IPP,i}^2$ are measurement error variances, and the $\overline{\Delta}_{bias,i,j}^2$ are covariances that specify the correlation of bias errors between vertical delay measurements made with common satellites or common receivers.

B. Ionospheric irregularity detection

Under nominal ionospheric conditions, the accuracy of fits based upon the thin-shell model has been found sufficient to meet WAAS performance requirements. Under disturbed conditions, however, the relationship between slant and vertical delay is often modeled poorly by the thin-shell approximation. To ensure the integrity of the broadcast delay and its confidence bound, it is imperative to determine whenever such a model does *not* accurately describe ionospheric behavior. In WAAS this issue is addressed by introducing an *irregularity detector* based upon the χ^2 of the planar fit (see Walter et al., 2000). The χ^2 of the fit may be written as follows:

$$\chi^2(\mathbf{a}; \mathbf{W}) = [\mathbf{y} - \mathbf{G} \cdot \mathbf{a}]^T \cdot \mathbf{W} \cdot [\mathbf{y} - \mathbf{G} \cdot \mathbf{a}], \quad (7)$$

where all quantities have been defined in the previous section. The presence of a significant irregularity is declared whenever the χ^2 exceeds a specified threshold χ_i^2 that depends upon the number of observations used in the fit. When this occurs, the ionosphere is no longer assumed to exhibit nominal behavior in the vicinity of the IGP, and the bound on the broadcast delay error at the IGP is raised to a maximum limit.

C. Ionospheric storm detection

The concept of local irregularity detection described above can be readily extended to address regional ionospheric storm detection. Since the impact of extreme storms is spread over a wide geographic area, the extreme storm detector is based upon a storm metric evaluated over an extended region. Periods of extreme storms can be defined in terms of thresholds and confirm intervals. The onset of an extreme storm is confirmed after the storm metric has crossed the *onset threshold* from below and remained above it for a specified *onset confirm interval*. Similarly, a storm clear is declared when the storm metric has crossed a *recovery threshold* from above and remained below it for a *recovery confirm interval*.

A particularly simple example is to define the instantaneous regional storm disturbance metric as the maximum of the ratio of χ^2 to χ_i^2 over the region of interest. Figure 2 shows fairly typical behavior for this metric as a function of time during an extreme storm over the WAAS service region. Note that by using this metric the fit at a single IGP can trip the extreme storm detector. It is found in practice, however, that whenever χ^2 / χ_i^2 crosses the onset threshold at one IGP, its value at many neighboring IGPs is near the onset threshold as well. This is undoubtedly due, not only to the wide impact of the extreme storm, but also to the fact that fits at neighboring IGPs share many of the same observations (*i.e.*, the domain of each fit covers many IGPs).

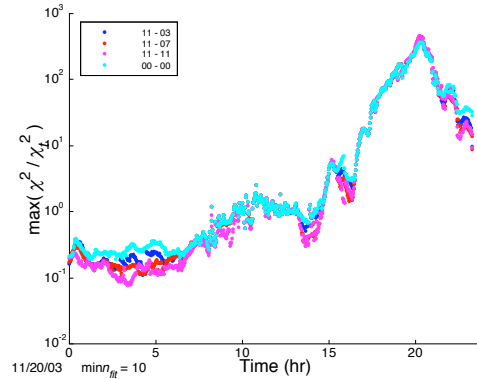


Fig. 2. The ionospheric storm metric as a function of time for the storm day of November 20, 2003. (The labels 11-03, 11-07, 11-11, and 00-00 refer to data-deprivation with, respectively, the 3, 7, 11, and 0 southern-most WRSs removed from the fit (see Section III-C).

Ionospheric storms can be ranked according to the maximum metric magnitude attained during the course of the storm. Figure 3 shows the range of maximum values that this metric achieves for a representative set of storms of the current solar cycle, including the most severe that have occurred. Here χ_i^2 is the value of the χ^2 distribution such that the probability of χ^2 exceeding this value is 10^{-3} for a fit with $N-3$ degrees of freedom, where N is the number of points

in the fit. Note that the horizontal axis uses a log scale. The most severe storms attain metric values that are nearly two orders of magnitude larger than those of more modest storms. Such a metric is therefore a good candidate for distinguishing *extreme* storms.

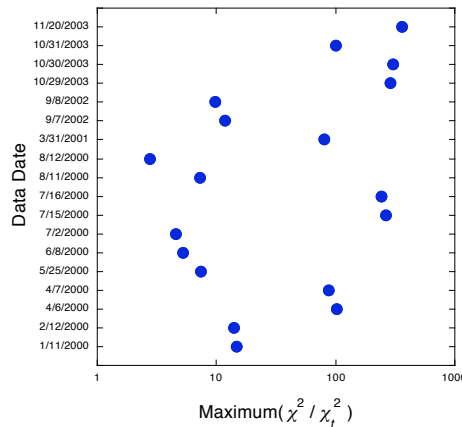


Figure 3. The maximum storm disturbance metric value achieved over distinct days (24 hour days UTC) during which ionospheric storms occurred.

We have investigated other possible storm metrics as well. Metrics based upon the local planar fit have included:

- (1) the sum of σ^2 / σ_t^2 over the entire grid;
- (2) the maximum sum of σ^2 / σ_t^2 at IGPs within 800, 1400, and 2000 km;
- (3) the sum of the log of σ^2 / σ_t^2 over the entire grid;
- (4) the maximum sum of the log of σ^2 / σ_t^2 at IGPs within 800, 1400, and 2000 km;
- (5) the maximum fit vertical delay over the entire grid;
- (6) the sum of fit vertical delays over the entire grid;
- (7) the maximum sum of fit vertical delays at IGPs within 800, 1400, and 2000 km;
- (8) the sum of the log of fit vertical delays over the entire grid; and
- (9) the maximum sum of the log of fit vertical delays at IGPs within 800, 1400, and 2000 km.

Metrics based upon observed delays have included:

- (1) the maximum vertical delay at IGPs within 800, 1400, and 2000 km;
- (2) the maximum mean vertical delay at IGPs within 800, 1400, and 2000 km; and
- (3) the maximum mean vertical delay of the top 25% at IGPs within 800, 1400, and 2000 km.

We have found that metrics based directly upon ionospheric delay (either observed or estimated) do not distinguish extreme storms from more moderate storms as readily or reliably as the ones based upon the ratio of σ^2 to σ_t^2 . While many of the latter perform well, little appears to be gained by the added complexity of any of these metrics relative to the one used to generate Fig. 1. Thus, the maximum ratio of σ^2 to σ_t^2 over the entire IGP grid has been selected as the storm metric for the operational WAAS system.

III. The Ionospheric Threat Model

As the ionosphere becomes increasingly disturbed, the residual error associated with a planar fit rises, indicating that delay estimates based upon this fit are less reliable. Consequently, the broadcast confidence bounds must be increased or, alternatively, when fit residuals become sufficiently large, the fit must be declared unusable and the error bound set to a maximum limit. As long as fit residuals accurately reflect the degree of disturbance of the ionosphere, confidence in the reliability of the broadcast error bounds remains high. Ionospheric irregularities that escape detection, however, represent a potentially serious threat to the integrity of this process. To protect the user from the threat posed by undersampling, WAAS employs an *ionospheric threat model* consisting of tabulated corrections that augment the confidence bounds of the delay estimates. In this section we first review how the ionospheric threat model is derived,

emphasizing modifications that are planned for the next WAAS upgrade, and then we examine how implementation of an extreme storm detector affects this threat model.

A. GIVE

The variance upon which the broadcast grid ionospheric vertical error (GIVE) is based is a function of measurement error, the uncertainty associated with the plane of the fit, and threat model contributions that protect against undersampling. In its Initial Operating Capability (IOC), WAAS has separated the ionospheric threat model into two distinct parts: the *spatial* threat model and the *temporal* threat model. The spatial threat model deals with the *instantaneous* threat posed by undersampled irregularities. The temporal threat model provides adjustment of the error bounds to account for the growth of irregularities between evaluations of planar fits. In the next WAAS upgrade, these distinct contributions to the GIVE will be replaced by a single contribution from a combined spatial-temporal threat model.

In the updated algorithm, the GIVE variance may be written:

$$\sigma_{GIVE}^2 = \sigma_{IGP}^2 + \sigma_{undersamp}^2, \quad (8)$$

where σ_{IGP}^2 is the (inflated) formal error variance due to measurement noise and the uncertainty of the fit plane, and $\sigma_{undersamp}^2$ is the augmentation of the variance required to protect against undersampling. In this equation, we have ignored any augmentation of the error to account for a possible azimuth and elevation dependent bias in pseudo-range measurements due to group delay variation from the antenna element. Derivations of expressions for antenna bias maximum error and σ_{IGP}^2 are subjects beyond the scope of this paper

B. Calculation of $\sigma_{undersamp}$

To determine $\sigma_{undersamp}^2$, the threat model contribution to the GIVE, we first tabulate the maximum error associated with undersampled irregularities as a function of two metrics that characterize the distribution of IPPs about the IGP. In the current implementation, these metrics are the fit radius and the ratio of the centroid radius to the fit radius, designated the *relative centroid metric*, where the centroid radius is the distance from the IGP to the centroid of the IPPs included in the fit. The quantity tabulated is

$$\text{raw} \sigma_{undersamp} = \max \left[\sqrt{\frac{A_{inflation}^2 |I_{\square,IPP} - \hat{I}_{\square,IPP}|^2}{K_{undersamp}^2}} \sigma_{IGP}^2 \right] \quad (9)$$

where $I_{\square,IPP}$ is an observed slant delay value projected to vertical, $\hat{I}_{\square,IPP}$ is the corresponding estimate of this value derived from the fit, $K_{undersamp}$ is a constant that translates a given maximum to a one-sigma value of a Gaussian distribution, and $A_{inflation}$ is a residuals inflation factor (taken to be 1.25 in the results presented below). $K_{undersamp}$ is specified by assuming that the tabulated (inflated) maximum is a 5 sigma-number, *i.e.*, $K_{undersamp} = 5.33$. Under nominal conditions, the radicand in eq. (9) will be negative for all data points, in which case the left-hand side is set to zero. Thus, we tabulate data only for days on which ionospheric storms have occurred. Furthermore, data are tabulated only for fits that fail to trip the irregularity detector.

In the IOC threat model, $\text{raw} \sigma_{undersamp}$ was evaluated only for delay estimates corresponding to observations belonging to the same epoch as the fit. In the updated GIVE algorithm, a combined spatial-temporal threat model is employed, where $\text{raw} \sigma_{undersamp}$ is evaluated for delay estimates over a fixed duration extending beyond the epoch of the fit. The new algorithm currently employs two such durations extending 470 and 770 seconds, respectively, past the fit epoch. The results presented below will refer only to the first duration.

Once the final tabulation of the $\text{raw} \sigma_{undersamp}$ is complete, an additional margin of safety is introduced by applying a two-dimensional overbound. Since in general, residual error will increase as the fit radius and relative centroid increase (*i.e.* as the distribution of IPPs becomes increasingly sparse and non-uniform), we require that the final $\sigma_{undersamp}$ be monotonically increasing as a function of each metric, *i.e.*,

$$\square_{undersamp}(R_{fit}, RCM) = \max_{r_{fit} < R_{fit}, r_{cm} < RCM} \left(r_{raw} \square_{undersamp}(r_{fit}, r_{cm}) \right). \quad (10)$$

Consequently, the spatial-temporal threat model is completely determined by a set of critical points at which the value of $\square_{undersamp}$ jumps upward when crossing to the next bin along each metric coordinate.

C. Data-deprivation

Two distinct types of threats posed by undersampled irregularities have been identified: (1) an irregularity occupying a region that coincides with a gap in the IPP coverage, and (2) an irregularity that resides at the edge of the WAAS service domain. To ensure that the user is protected adequately, we tabulate $r_{raw} \square_{undersamp}$ using data-deprivation to simulate multiple examples of such threats using the same set of observational data. For each IGP, various masks are employed to select IPPs to be removed from fits and subsequently treated as possible user measurements. Residual error is then tabulated by comparing predicted and actual delay values for the excluded observations that lie near the IGP. Note that the data-deprivation schemes used to generate the IOC threat model differ from those of the next WAAS upgrade as the latter, described below, have been found to be more representative of configurations of IPPs actually encountered in the system.

Irregularities in gaps are simulated by *single station deprivation*, *i.e.*, excluding IPPs associated with a single WAAS reference station (WRS). Single station deprivation is performed sequentially by removing one WRS at a time until all the WRSs have been considered. As an added measure of safety, one- and two-point *malicious* deprivation is performed on fits that initially trip the irregularity detector. *Malicious* deprivation consists of re-evaluating a fit after having removed the IPP that generates the largest fit residual. Removing one or two carefully selected points is sometimes sufficient to reduce the \square^2 of the fit below the irregularity detector threshold.

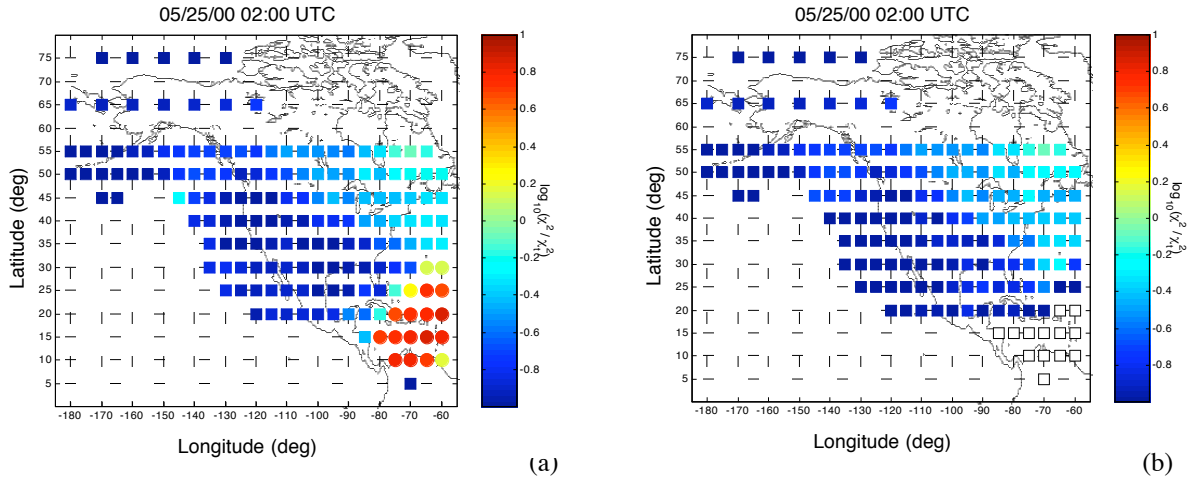


Figure 4. The magnitude of \square^2 / \square_i^2 at each WAAS IGP at 2:00 UTC, May 25, 2000, for (a) no data-deprivation, and (b) removing data associated with the 11 southern-most WRSs. Colored squares and circles indicate where this ratio is, respectively, below and above an irregularity detector threshold value of 1. (Empty squares indicate where an insufficient number of observations were available to perform a fit.)

Irregularities at the edge of service are simulated by *directional station deprivation*, *i.e.*, removing up to 13 WRSs that occupy the furthest extreme in a particular direction from the IGP. Eight directions are examined: north, south, east, west, northeast, northwest, southeast, and southwest. Figure 4 illustrates the effect of removing the eleven southern-most WRSs. The presence of an irregularity over southern Florida and Cuba is clearly visible in Fig. 4(a). If the irregularity had occurred further south (moving the edge of the WAAS service domain northward is equivalent to moving the irregularity southward), however, it might have gone undetected as indicated in Fig. 4(b).

It should be emphasized that the trip times of the extreme storm detector used to generate the threat model are dependent upon the data-deprivation scheme employed. Under severe data-deprivation, the presence of an extreme storm may not be detected (as indicated by Fig. 4). When this occurs, however, the potentially large contributions to the threat

model that might arise from the region of disturbance have been either excluded by the data-deprivation or relegated to a region of the threat model characterized by poor IPP coverage (*i.e.*, large fit radius and/or large relative centroid),

D. Supertruth

To define a representative threat model, we have tabulated $\sigma_{undersamp}$ for days on which moderate to severe ionospheric storms occurred. These data consist of post-processed slant delay measurements collected by the existing 25 WAAS Reference Stations. The objective of the post-processing is to eliminate interfrequency biases, to remove the effects of cycle slips in carrier phase measurements, to level the carrier phase measurements to the corresponding range measurements, and to detect and eliminate spurious measurements using the redundancy provided by having three receivers at each site. Such data, designated *supertruth*, contain minimal error, and this error is due primarily to multipath and receiver noise. It should be noted that the older supertruth data (data processed prior to 2003) have been reprocessed to restore a large fraction of the observations that had previously been eliminated. The new versions of the supertruth files used to generate the IOC threat model are up to 50% larger.

E. The impact of the extreme storm detector on the threat model

Figure 5 shows the effect of excluding from the threat model fits that occur during extreme ionospheric storms. Data from the following 14 storm days have been processed:

1/11/2000	4/6/2000	4/7/2000	7/15/2000	7/16/2000
3/31/2001	10/21/2001	11/6/2001	11/24/2001	10/29/2003
10/30/2003	10/31/2003	11/20/2003	11/21/2003	

Figure 5(a) shows $\sigma_{undersamp}$ as a function of the two IPP coverage metrics when all data are processed. Figure 5(b) shows the corresponding threat model when fits are excluded during periods of extreme storms. To generate the latter result, we have used the following parameters to define the storm periods during which fits are excluded:

onset threshold:	$\sigma^2 / \sigma_{lowerbound}^2 = 50$
onset confirm interval:	1 hour
recovery threshold:	$\sigma^2 / \sigma_{lowerbound}^2 = 45$
recovery confirm interval:	8 hours

A distinct set of extreme storm trip times is calculated for each data-deprivation mask. Using these thresholds is found to remove from the threat model many hours of data for ten out of the fourteen storm days processed (as can be seen, for example, in Fig. 2).

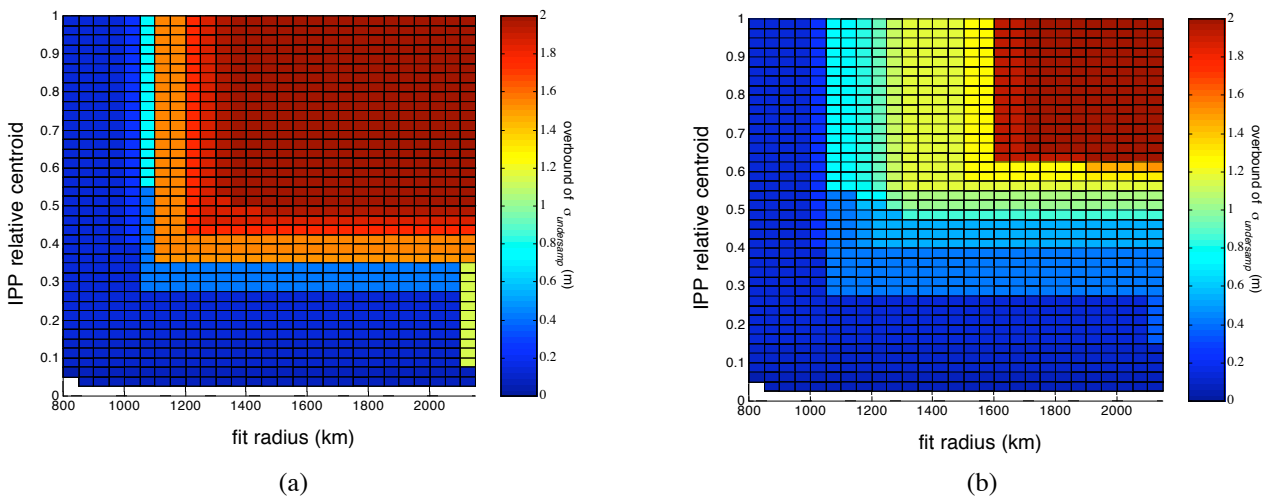


Figure 5. Ionospheric threat model (a) before and (b) after implementing the extreme storm detector.

This computation differs in some respects from the one that will be used to generate the actual upgrade of the WAAS ionospheric threat model. First, to reduce the time of computation, our calculation evaluates delay estimates

using an epoch spacing of 100 seconds rather than 10 seconds (however, in both threat models, fits are evaluated only every 100 seconds). Secondly, it simplifies the computation somewhat to perform fits at IPP locations (treated as pseudo-IGPs) rather than at the WAAS IGP. Finally, we have not incorporated into the threat model any added protection against the threat posed by user pseudorange smoothing. Despite these differences, we expect our result to be representative of the FOC threat model. By excluding fits in periods of extreme storms, $\square_{undersamp}$ has been dramatically reduced over much of the threat model domain.

Summary

Implementing an extreme storm detector in WAAS should provide improvements in system safety and availability. The detector is based upon a storm metric derived from the \overline{f} of the fit at each IGP over the region of interest. It protects the user from the effects of undersampling dense, highly localized ionospheric irregularities that have been observed to occur during the recovery periods of extreme storms. It also provides protection against the impact of future storms that have magnitudes larger than those used in the generation of the ionospheric threat model. By relying on this detector to notify the system whenever an extreme storm occurs, the ionospheric threat model need only address threats that arise under moderate storm conditions. This permits a reduction in the amount by which broadcast confidence bounds are augmented to account for undersampling and, consequently, an improvement in system availability.

Acknowledgements

The research described in this paper was performed by the Jet Propulsion Laboratory, California Institute of Technology, under contract with the National Aeronautics and Space Administration. We also wish to acknowledge the contributions of our colleagues at Raytheon who have helped to develop the ideas presented in this paper, in particular, Daniel Cormier, Michael Gran, Nitin Pandya, Stephen Peck, Helena Eldridge, and Bao Nguyen.

References

- Altshuler, E., R. Fries, and L. Sparks, "The WAAS Ionospheric Spatial Threat Model," in **Proceedings of ION GPS 2001**, Salt Lake City, UT, September 11-14, 2001.
- Komjathy, A., L. Sparks, A.J. Mannucci and A. Coster, "The Ionospheric Impact of October 2003 Storm Event on WAAS", **Proceedings of ION GNSS 2004**, Long Beach, CA, Sept 21-24, 2004.
- Sparks, L., X. Pi, A.J. Mannucci, T. Walter, J. Blanch, A. Hansen, P. Enge, E. Altshuler, R. Fries, "The WAAS Ionospheric Threat Model," in **Proceedings of the International Beacon Satellite Symposium 2001**, Boston, College, Boston, June 3-6, 2001.
- Walter, T., A. Hansen, J. Blanch, P. Enge, A. Mannucci, X. Pi, L. Sparks, B. Iijima, B. El-Arini, R. Lejeune, M. Hagen, E. Altshuler, R. Fries, A. Chu, "Robust Detection of Ionospheric Irregularities," **Proceedings of the International Beacon Satellite Symposium 2001**, Boston, College, Boston, June 3-6, 2001.